

# Measurement of the plasma edge profiles using the combined probe on W7-X

P. Drews<sup>1</sup>, Y. Liang<sup>1</sup>, S. Liu<sup>1</sup>, A. Krämer-Flecken<sup>1</sup>, O. Neubauer<sup>1</sup>, J. Geiger<sup>2</sup>, M. Rack<sup>1</sup>, M. Dostal<sup>1</sup>, D. Nicolai<sup>1</sup>, O. Grulke<sup>2</sup>, N. Wang<sup>1</sup>, A. Charl<sup>1</sup>, B. Schweer<sup>1</sup>, P. Denner<sup>1</sup>, Y. Gao<sup>1</sup>, K. Hollfeld<sup>3</sup>, G. Satheeswaran<sup>1</sup>, N. Sandri<sup>1</sup>, D. Höschen<sup>1</sup> and the W7-X Team<sup>1</sup>

<sup>1</sup>Forschungszentrum Jülich GmbH, Institut für Energie- und Klimaforschung Plasma-physik, Partner of the Trilateral Euregio Cluster (TEC), 52425 Jülich, Germany

<sup>2</sup>Max-Planck-Institut für Plasmaphysik, Greifswald, Germany

<sup>3</sup>Forschungszentrum Jülich GmbH, Central Institute for Engineering, Electronics and Analytics/Engineering and Technology (ZEA-1), 52425 Jülich, Germany

*Corresponding Author:* p.drews@fz-juelich.de

## Abstract:

Wendelstein 7-X (W7-X), started operation in December 2015 with a limiter configuration. In conjunction with the multi-purpose manipulator, a fast reciprocating probe has been installed. This combined probe is able to measure the local electron temperatures and densities, magnetic field, the radial electric field and the plasma flow. These parameters are very useful in ascertaining the edge plasma performance. In addition, the fieldline tracing feature of the W7-X webservices was used to calculate the connection length along the path of the probe, for each configuration, to be compared to the measured profiles. Both, measured quantities and calculated connection lengths are used to determine the crossfield transport.

## 1 Introduction

Wendelstein 7-X (W7-X), one of the worlds largest optimized stellarators, located at the IPP Greifswald, started operation recently with a limiter configuration [1]. Both helium and hydrogen plasmas were produced, with discharge durations of up to 6 s and 4 MJ from electron cyclotron resonance heating (ECRH). Edge plasma profile measurements, especially those of the electron temperature and density, will play a key role in validating the performance in comparison to the tokamak and hence the viability of a stellarator fusion reactor. Part of this first campaign were studies on the configuration effects of the magnetic topology on the transport. It was a stated aim [2] to find a configuration that has a minimized neoclassical transport and also the powerloads on the limiter or divertor for future long pulse operation have to be optimized. The combined probe was employed together with the multipurpose manipulator to obtain plasma edge profiles. The abilities of the combined probe are to be compared with the reflectrometrie at the edge. The

paper describes the measurements conducted with the combined probe, section 1.1 will give details about the diagnostic, section 2 discusses the measurements using the combined probe and section 2.1 discusses the  $\iota$  dependency of the crossfield transport and the pressure decay length. In section 2.2 a comparison of the measurements of the radial electric field with the data from the reflectrometry is shown.

## 1.1 Experimental setup

A multi-purpose manipulator (MPM) was installed at the low field side of the vacuum vessel on W7-X in 2015 and commissioned in early February 2016 [4][5], in order to mount a wide variety of diagnostic probes for measurements of the plasma edge profiles and for plasma wall interaction studies. The first diagnostic to be used was the so-called combined probe. It is located in the midplane of module four at the AEK41 flange and able to plunge 35 cm into the vacuum vessel. The combined probe includes two 3D magnetic pick-up coil arrays (similar to those in [6]), five Langmuir probe pins [7], and a Mach setup [8]. This allowed to simultaneously measure, the edge radial profiles of the magnetic fields, the electron temperature and density, the electric field and the plasma flow. The Langmuir probe array consists of three floating potential pins, that deliberately differ in radial and poloidal position, for the calculation of the electric field and correlation of the radially and poloidally separated floating potential measurements. In addition, one pin is negatively biased in order to measure the ion saturation current  $I_{\text{sat}}$  and another pin is positively biased with voltage  $U_+$  to collect electrons.

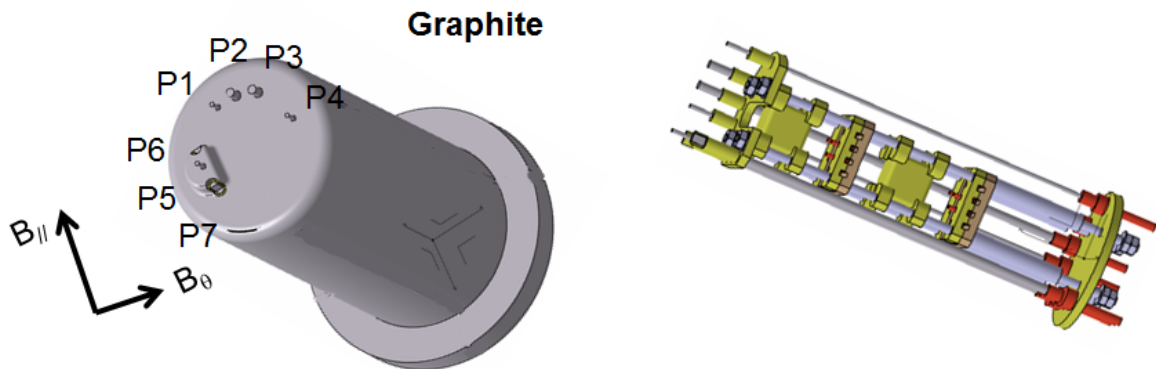


FIG. 1: Left: Sketch of the arrangement of the Langmuir and Mach probe pins with cover, right: interior of the combined probe

The Langmuir probe measurements yielded temperature, density and radial electric field profiles, in addition also time traces for the temperature and density and the plasma edge, with the MPM in fixed position, were recorded. The Langmuir probe shown in figure 1 contains three floating potential pins (P1, P4, P5), with pin P5 being on a stage 3 mm radially deeper. This arrangement of the floating potential pins was made to allow

turbulence studies via correlating the differently radially and poloidally placed probes. The measurements of the temperature and density were within reasonable agreement with the limiter Langmuir probes [3]. In addition one pin biased positively and another biased negatively is located on the top of the probe head. P6 and P7, are in parallel to the toroidal magnetic field direction and used as a Mach probe. The pick-up coils, shown in figure 1 on the right, are arrayed as a set of two 3D coils wound around each other, they are radially separated by 3.1 cm along the probe. The pick-up coils greatly increase the abilities of the probe since it allows measurements not only inside of the plasma but also at the vessel wall. The measured magnetic field profiles match the calculated ones as shown in [10].

## 2 Measurements

The iota configuration was changed by tuning the planar coils according to table I, the measurements were performed at under the same ECRH heating of 2.7 MW. The machine performance had considerably improved with the conditioning, such that the line averaged densities were consistent throughout the day. It is clearly visible in the density and temperature profiles (see figure 2), that the magnetic axis and therefore also the last closed flux surface (LCFS) was shifted. The density profiles show in addition the exponential fit function used to determine the decay length. It was assumed that  $T_e = T_i$  for the

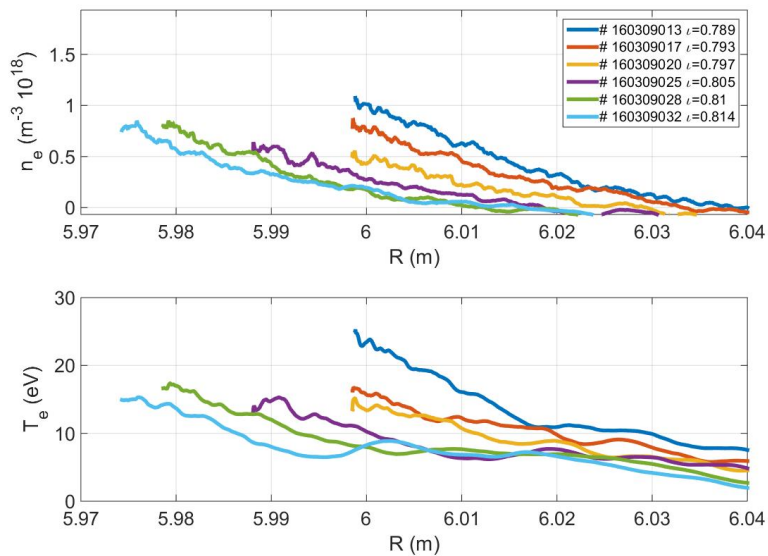


FIG. 2: Temperature and density profiles of the iota scan

calculation of several quantities, since for first campaign no diagnostic was operational that could measure the ion temperature in the same detail as the Langmuir probes did for the electrons.

TABLE I: COIL CONFIGURATIONS FOR THE IOTA SCAN

Scenario #	Index	I1,I2,I3,I4,I5 (A)	IA (A)	IB (A)
20160309.013	conf. J	12370	4824	4824
20160309.017	iota 3	12383	4829	3622
20160309.020	iota 5	12391	4832	2819
20160309.025	iota 9	12408	4839	1210
20160309.028	iota 11	12412	4841	807
20160309.032	iota 13	12420	4844	0

## 2.1 Iota dependency of the transport

The connection length for the chosen scenarios shown in figure 3 indicates a similar shift of the profiles. The calculated connection lengths needed sliding average filtering as small island like structures could lead to wrong values. The W7-X fieldline tracing webservice [11] was used to calculate the connection length along the path of the combined probe. The transport of both ions and electrons is strongly dependent on the connection length as it is inversely proportional to the connection length [12]. It is also evident that tuning the

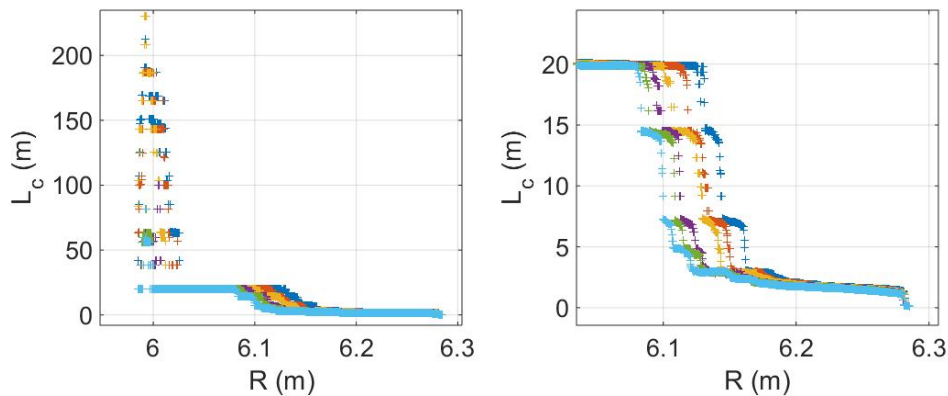


FIG. 3: Connection length calculated for the iota scan, left: full range of the manipulator, right: magnified at the last closed surface

planar coils, shifts the last closed surface successively inwards, visible in the connection length and the density and temperature profiles. The higher iota configurations experience a much smaller spike in the connection length at about  $R = 6$  m. The density decay length  $\lambda_{n_e}$  was obtained from:

$$n_e(r) = n_0 \exp\left(\frac{r - R_0}{\lambda_{n_e}}\right). \quad (1)$$

For the regression analysis to represent the data starting from the last closed flux surface the appropriate time range of the position data was used in addition a threshold value

of  $n_e = 5 \cdot 10^{16} \text{ m}^{-3}$  for the density was used. This was necessary as the electron density experienced slightly negative values just before entering the plasma, this is assumed to be caused by fast electrons. The crossfield particle transport can be calculated using [12]:

$$D_{\perp} = \frac{\lambda_{n_e}^2 c_s}{L_c}. \quad (2)$$

With  $c_s \approx \sqrt{\frac{2T_e}{m_i}}$  as the ion sound speed and  $L_c$  the calculated connection length. The challenge presented here is the right choice of initial parameters for the fit since, with the tuning of the planar coils the last closed surface is expected to be moving inwards.

The neoclassical diffusion coefficients were calculated using [13]:

$$D_{\text{neo}} = 1.2 \cdot 10^{-21} \frac{n_e \ln \Lambda}{B^2 \sqrt{T_e}} (1 + 2/\iota^2). \quad (3)$$

Figure 4 shows the results for the calculation of the crossfield and neoclassical diffusion coefficients. The electron pressure is calculated using the temperature and density profiles,

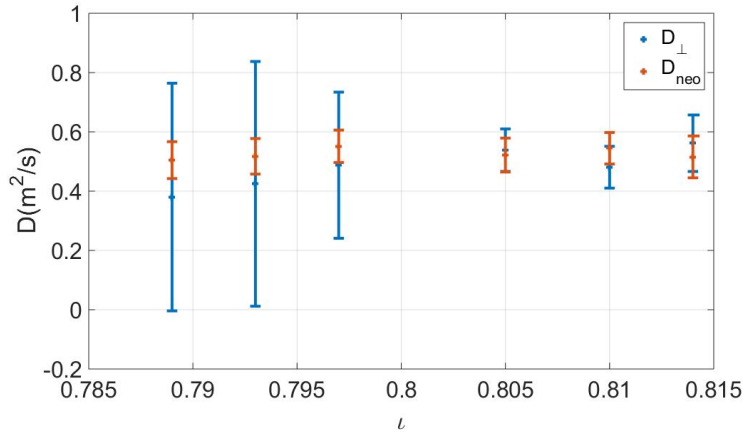


FIG. 4: Neoclassical diffusion coefficients for the iota scan

by multiplying  $n_e$  and  $T_e$ . From this electron pressure profile the power decay length  $\lambda$  is deduced using:

$$p_e(r) = p_0 \exp\left(\frac{r - R_0}{\lambda_{p_e}}\right). \quad (4)$$

Figure 5 shows the pressure profiles and the fitted functions, this pressure decay length is recognized as a crucial quantity concerning peak heat loads [14]. On the right hand side the power decay length against the central iota value is plotted. The pressure decay length was obtained from the fit of the data on the right and the error is taken from the 85 % confidence bound. For the fit to represent to data starting from the last closed flux surface a threshold value of  $n_e = 5 \cdot 10^{16} \text{ m}^{-3}$  for the density was used to choose the appropriate range past the last closed surface. The values from the experiment show that

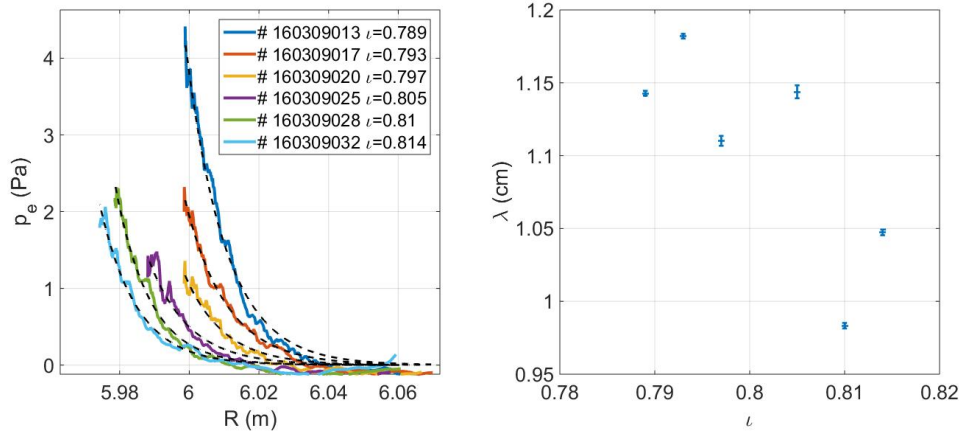


FIG. 5: Left: pressure profiles of the iota scan, right: power decay length obtained from fit versus central iota

the decay length stays constant with increasing iota to a maximum value for  $\iota = 0.805$  and then sharply decreases. These findings have to be compared to the measured heat loads on the limiter, but again here the increased distance due to the inwards shift has to be taken into account.

## 2.2 Comparison of the radial electric field $E_r$

The radial electric field was measured using the floating potential pins which were  $\Delta R = 3$  mm radially apart. The radial electric field is calculated using:

$$E_r = -\frac{\partial(U_{\text{float}} + 2.8 \cdot T_e)}{\partial r} = -\left(\frac{U_{\text{float-up}} - U_{\text{float-down}}}{\Delta R} + 2.8 \frac{T_e(r + \Delta r) - T_e(r)}{\Delta r}\right). \quad (5)$$

It is necessary here to take the  $T_e(r)$  from the profile, since there are not two independent temperature measurements in different radial positions. The selection using a low pass filter with a cut-off frequency of 50 Hz was necessary to obtain the data. The values of the electric field from the combined probe close to its final position are prone to error as the  $1/\Delta r$  term becomes very large. The measurements of the radial electric field can be compared to those of the reflectrometry [15]. The ability to compare the results of those two diagnostics depend mostly on the plasma density profile, as it defines the penetration of the reflectrometry. The reflectrometry and the MPM are not in the same toroidal position. Figure 6 shows the two radial electric field signals for a shot with a very far outreaching reflectrometry measurements and two deepest Langmuir probe measurements. The two diagnostics have a different range, the combined probe is limited to the very edge of the plasma while the reflectrometry measurements depending on the density and operation frequency can go as deep as the core. The Langmuir probe measurements consistently yield a lower but still positive value for the radial electric field compared to the reflectrometry.

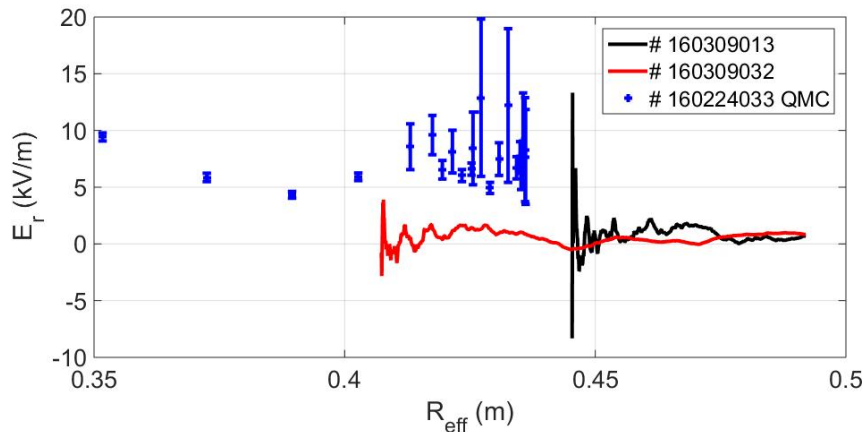


FIG. 6: Radial electric field measured with the combined probe (solid line) and reflectrometry (dots)

### 3 Summary and Outlook

The combined probe was successfully able to measure the edge plasma profiles for the electron temperature, density, radial electrical field and magnetic field. The measurements of the Langmuir probe mounted on the manipulator is in good agreement with the limiter Langmuir probes and the magnetic profiles agree with the calculated values. It is possible to determine the transport by combining these measurements. The measurements of the radial electric field using the combined probe do not entirely agree with the results from reflectrometry. The data from the Langmuir probes is well agreeing with the measurements from the limiter Langmuir probes. The existing probe will be improved upon concerning the arrangement of the floating potential pins for correlation measurements, the Mach probe pins will have their ceramic insulator on the plasma facing side removed to prevent any possible leak currents and a dedicated Mach probe array and a retarding field analyzer will be employed in the second operational phase.

### References

- [1] DINKLAGE A., Confinement in Wendelstein 7-X Limiter Plasmas, Proceedings of the 43nd EPS, (2016)
- [2] KLINGER T., Performance and properties of the first plasmas of Wendelstein 7-X Proceedings of the 43nd EPS, (2016)
- [3] KRYCHOWIAK M. et al., Overview of diagnostic performance and results for the first operation phase in Wendelstein 7-X, submitted HTPD 2016
- [4] NICOLAI D. et al., A Multi-Purpose Manipulator system for W7-X as user facility for plasma edge investigation submitted SOFT 2016

- [5] SATHEESWARAN G. et al., vA PCS7 -based control and safety system for operation of the W7-X Multi-Purpose Manipulator facility submitted SOFT 2016
- [6] YANG Y. et al., Experimental observations of plasma edge magnetic field response to resonant magnetic perturbation on the TEXTOR Tokamak Nucl. Fusion **52** 074014 (2012)
- [7] TONKS and LANGMUIR, A General Theory of the Plasma of an Arc Phys Rev. **34**, 876-922 (1929)
- [8] CHUNG K., "Mach probes" Plasma Sources Sci. Technol. **21**, 063001 (2012)
- [9] CHEN S. and SEKIGUCHI T., Instantaneous DirectDisplay System of Plasma Parameters by Means of Triple Probe J. Appl. Phys. **36**, 2363 (1965)
- [10] DREWS P., Preliminary results on the measurement of plasma edge profiles using the combined probe on W7-X" Proceedings of the 43rd EPS, (2016)
- [11] BOZHENKOV S., Service oriented architecture for scientific analysis at W7-X. An example of a field line tracer, Fusion Engineering and Design **88** (2013) 2997 3006
- [12] KÓCAN M., Ion temperature measurements in the scrape-of layer of the Tore Supra tokamak, Université Henri Poincaré (2009)
- [13] STROTH U., Plasmaphysik, Vieweg+Teubner (2011)
- [14] EICH T., Inter-ELM Power Decay Length for JET and ASDEX Upgrade: Measurement and Comparison with Heuristic Drift-Based Model PRL. **107**, 215001 (2011)
- [15] KRÄMER-FLECKEN A. et al., Investigation of turbulence rotation in limiter plasmas at W7-X with a new installed Poloidal Correlation Reflectometry, in this conference.

## Acknowledgements

*The author would like to thank B. Stanley of the IPP Greifswald for setting up and explaining the data acquisition system at W7-X for the multi-purpose manipulator and P. Sinha and H. Niemann of the IPP Greifswald for helping with debugging the connection length calculation.*

*This work has been carried out within the framework of the EUROfusion Consortium and has received funding from the Euratom research and training programme 2014-2018 under grant agreement No 633053. The views and opinions expressed herein do not necessarily reflect those of the European Commission.*